Understand flaws in communication cable production thanks to balunless single-ended measurements

By Peter Fischer, AESA SA Switzerland, www.aesa-cortaillod.com

Balunless cable measurement technique opens the door to many new parameters, most of them not well-known or misunderstood. For the upcoming 40GBase-T application (IEEE 802.3bq) a deeper understanding of these new opportunities in measurement technology is essential to reduce development time, improve quality and discover weeknesses.

Abstract

This paper presents new opportunities in measurement technology to help data cable manufacturer finding the cause of marginal or failing lots in production by analysing single-ended S-parameters which can be accessed by balunless test method.

This method allows by mathematical superposition of single-ended measurements to get the well-known mixed-mode S-parameters.

In case of faults an analysis of the respective single-ended S-parameters can help finding the cause fast and efficiently. Several examples of such analysis are presented.

Introduction

Traditionally data cables are tested with a balun at each end of the cable. The limited bandwidth was sufficient for lower categories and common and mixed-mode S-parameters not required or difficult to evaluate.
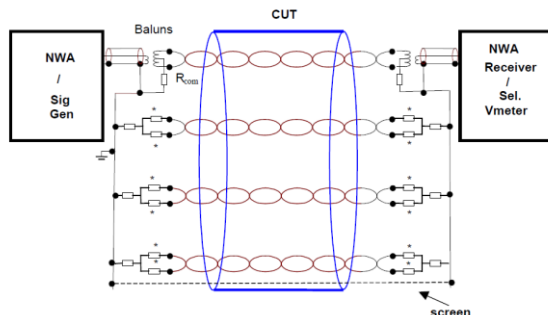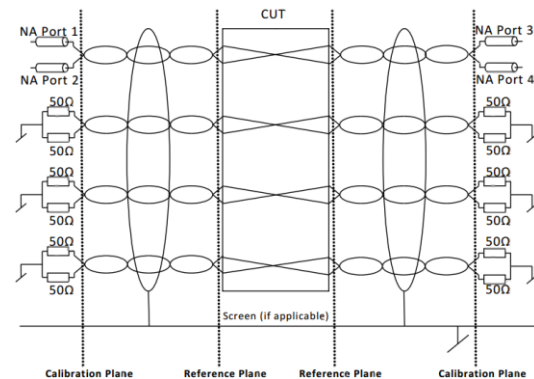

[i] Example of balun testing: Insertion Loss

At higher maximum frequency these parameters get more and more important. According to IEC 61156-5 balance requirements are given only up to 250 MHz because of balun restrictions.

In the meantime the industry rediscovered the symmetry parameters again because a higher percentage of failures could be traced back to TCL and EL TCTL.

[ii] Example of balunless testing: Insertion Loss

In the drawings above the same Insertion Loss measurement is shown, as an example.

The most obvious point beside the use of baluns or not is the number of VNA ports which are needed to get the same S-parameter. More ports means also more sweeps leading to a longer test time.

What is the reason why balunless testing should be in preference?

We will see later that in the same sweep we get not only the well-known differential-mode Insertion Loss S_{dd}, but also the common-mode Insertion Loss S_{cc}, the single-ended Insertion Loss S_{13} and S_{24} as well as the in pair FEXT S_{14} and S_{23}.

Theoretical background

As described by Fan et al (2003), the key is a conversion of single-ended S-parameters into mixed-mode S-parameters.
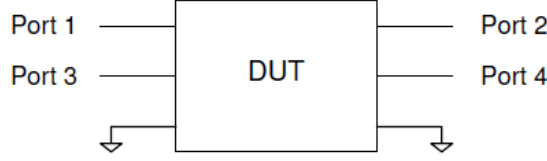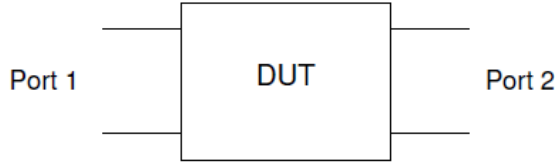

iii 4-Port device (single-ended)

Therefore the 4-Port device can be mathematically represented by single-ended S-parameters and the waves going into the DUT (a) and the waves which come out of the DUT (b).

$$\begin{bmatrix} b_1 \\ b_2 \\ b_3 \\ b_4 \end{bmatrix} = \begin{bmatrix} S_{11} & S_{12} & S_{13} & S_{14} \\ S_{21} & S_{22} & S_{23} & S_{24} \\ S_{31} & S_{32} & S_{33} & S_{34} \\ S_{41} & S_{42} & S_{43} & S_{44} \end{bmatrix} \begin{bmatrix} a_1 \\ a_2 \\ a_3 \\ a_4 \end{bmatrix}$$

iv Single-ended matrix representation

In a similar way the same DUT can be represented as a 2-Port differential device:

v 2-Port differential device (mixed-mode)

A mixed-mode S-matrix can be organised similarly to the single-ended S-matrix:

$$\begin{bmatrix} b_{d1} \\ b_{d2} \\ b_{c1} \\ b_{c2} \end{bmatrix} = \begin{bmatrix} S_{dd11} & S_{dd12} & S_{dc11} & S_{dc12} \\ S_{dd21} & S_{dd22} & S_{dc21} & S_{dc22} \\ S_{cd11} & S_{cd12} & S_{cc11} & S_{cc12} \\ S_{cd21} & S_{cd22} & S_{cc21} & S_{cc22} \end{bmatrix} \begin{bmatrix} a_{d1} \\ a_{d2} \\ a_{c1} \\ a_{c2} \end{bmatrix}$$

vi 2-Port differential matrix representation

With comparison between both cases, single-ended and mixed-mode, the mathematical correlation for each mixed-mode S-parameter can be found and explained by a combination of 4 single-ended S-parameters.

The resulting mixed-mode S-matrix is consisting of differential-mode to differential-mode (yellow), common-mode to common-mode (green) and mixed-mode (common-mode to differential-mode (blue) and differential-mode to common-mode (pink)) S-parameters:

$$S_{mm} = \begin{bmatrix} S_{dd11} & S_{dd12} & S_{dc11} & S_{dc12} \\ S_{dd21} & S_{dd22} & S_{dc21} & S_{dc22} \\ S_{cd11} & S_{cd12} & S_{cc11} & S_{cc12} \\ S_{cd21} & S_{cd22} & S_{cc21} & S_{cc22} \end{bmatrix}$$

- ⬜ (yellow) Differential-mode to differential-mode
- ⬜ (blue) Common-mode to differential-mode
- ⬜ (magenta) Differential-mode to common-mode
- ⬜ (green) Common-mode to common-mode

vii Mixed-mode matrix

As a reading example the following formula can be taken:

$$RL_{dd} @\, Port\ 1 : S_{dd11} = \frac{1}{2}(S_{11} - S_{13} - S_{31} + S_{33})$$

$$S_{mm} = \frac{1}{2} \begin{bmatrix} \begin{bmatrix} S_{11} - S_{13} - S_{31} + S_{33} & S_{12} - S_{14} - S_{32} + S_{34} \\ S_{21} - S_{23} - S_{41} + S_{43} & S_{22} - S_{24} - S_{42} + S_{44} \end{bmatrix} & \begin{bmatrix} S_{11} + S_{13} - S_{31} - S_{33} & S_{12} + S_{14} - S_{32} - S_{34} \\ S_{21} + S_{23} - S_{41} - S_{43} & S_{22} + S_{24} - S_{42} - S_{44} \end{bmatrix} \\ \begin{bmatrix} S_{11} - S_{13} + S_{31} - S_{33} & S_{12} - S_{14} + S_{32} - S_{34} \\ S_{21} - S_{23} + S_{41} - S_{43} & S_{22} - S_{24} + S_{42} - S_{44} \end{bmatrix} & \begin{bmatrix} S_{11} + S_{13} + S_{31} + S_{33} & S_{12} + S_{14} + S_{32} + S_{34} \\ S_{21} + S_{23} + S_{41} + S_{43} & S_{22} + S_{24} + S_{42} + S_{44} \end{bmatrix} \end{bmatrix}$$

viii Transformation matrix between single-ended S-parameters and mixed-mode S-parameters
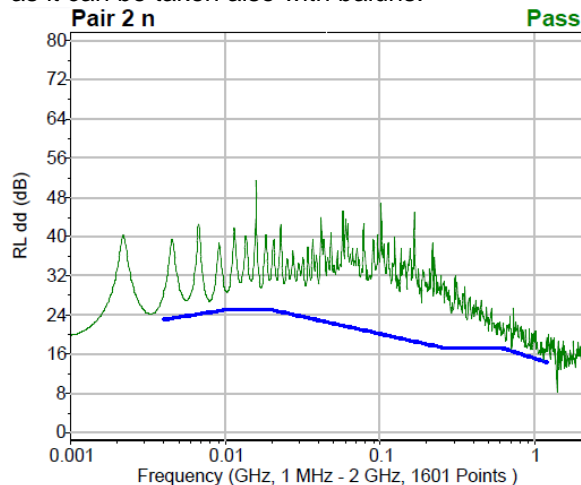
The transformation matrix is the base of the following discussion and analyses. Explanation to this formula and some others will be given in the following parts with examples.

Case 1: Low RL

As shown above the RL @ Port 1 is represented by S_{dd11}:

$$S_{dd11} = \frac{1}{2}(S_{11} - S_{13} - S_{31} + S_{33})$$

Here we have an example of RL measurement as it can be taken also with baluns.

Return Loss measurement of near end pair 2

The measurement shows a Pass with a marginal margin of 0.2 dB. For a cable manufacturer it can be ok but probably he was just lucky to get a Pass. For balun testing the story ends here. It is not possible to further evaluate the cause of the marginal measurement.

With the ability of balunless testing the cable manufacturer has much more opportunities to go deeper into single-ended measurements.

From the given formula for Return Loss we can find the 4 single-ended S-parameters. S_{11} and S_{33} are the single-ended Return Loss measurements of "a" wire and "b" wire of the pair. S_{13} and S_{31} are the crosstalk measurements from "a" wire to "b" wire and from "b" wire to "a" wire.
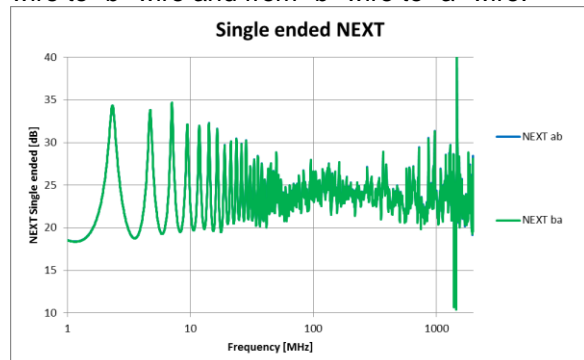
Single-ended NEXT measurements S_{13} and S_{31}
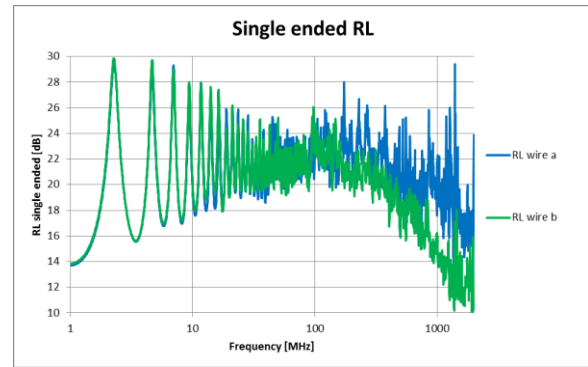
Single-ended RL measurements S_{11} and S_{33}

The overlay of the single-ended NEXT measurements S_{13} and S_{31} shows no noteworthy deviation over the whole frequency range. In contrast the single-ended RL measurements S_{11} and S_{33} show diverting values at 100 MHz and above.

These differences are causing the poor RL performance of near end. In this specific case wire "b" is worse than wire "a".

As written above there are even more opportunities with single-ended measurements. We can also compare the impedances of each wire.
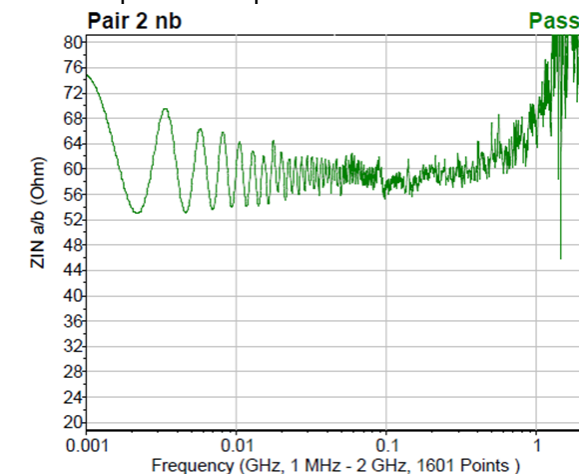
Increasing Impedance wire "b"

The final conclusion with access to single-ended S-parameters is imposed itself now:

The increasing impedance of wire "b" causes a bad single-ended RL performance which results in a bad differential-mode RL.

The access to single-ended S-parameters revealed the cause of poor performance which would stay completely hidden with balun based measurement technology.

AESA Cortaillod

Case 2: Failing TCL

If we consider our transformation matrix above we find for TCL (S_{cd11}) the following formula:

$$S_{cd11} = \frac{1}{2}(S_{11} - S_{13} + S_{31} - S_{33})$$

The example given below shows a well-known artefact in data cables, a peak in TCL. Today's balun based test equipment's are rarely providing access to the centre tap. This is caused by worse performance of the balun itself if this access is provided. Normally additional test equipment is required to do symmetry measurements.
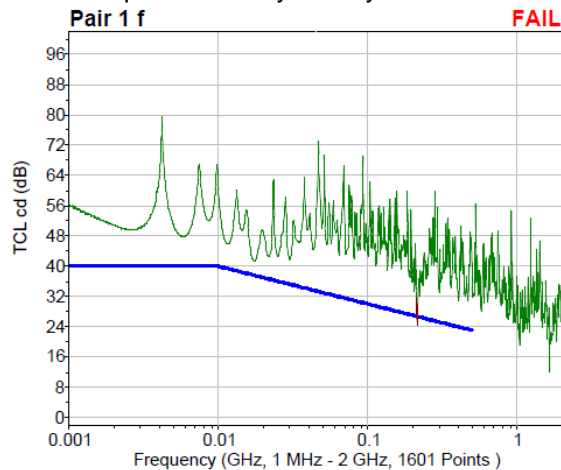

TCL measurement far end

Here we end with balun measurements. There is no way to find out what the cause of this peak is. Only single-ended measurements can provide the needed answers.

The formula above shows that the same S-parameters as for Return Loss are required. Only the algebraic signs are exchanged.

The comparison of the single-ended NEXT measurements S_{13} and S_{31} and the single-ended RL measurements S_{11} and S_{33} will give some further hints.
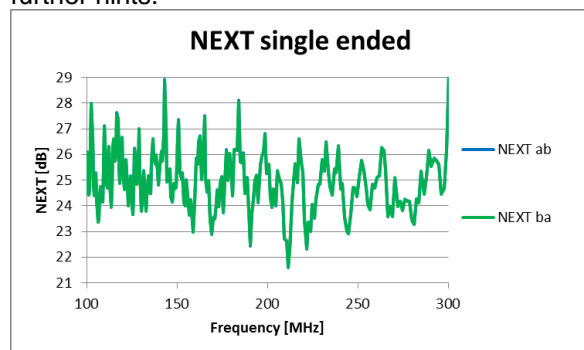

Single-ended NEXT measurements S_{13} and S_{31}

The overlay of both single-ended NEXT graphs shows a very similar behaviour in the frequency range near the peak which is at 210 MHz.
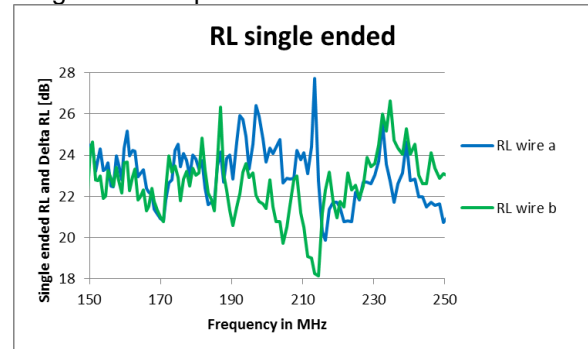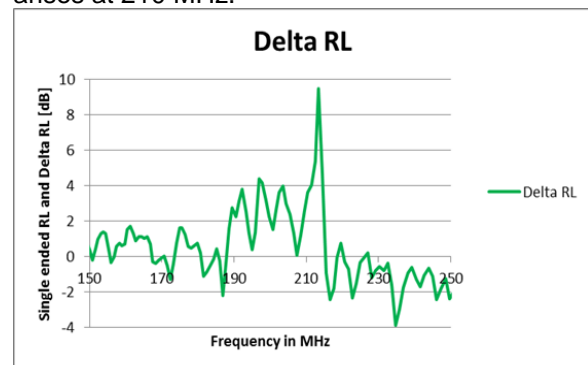

Single-ended RL measurements S_{11} and S_{33}

Single-ended RL shows a completely different picture. The differences are increasing between the 2 graphs at 200 MHz and result finally in two peaks in opposite direction at the frequency of the TCL peak.
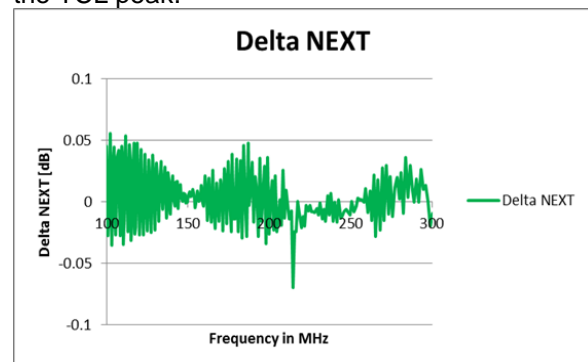

Difference of S_{13} and S_{31}

As expected, Delta NEXT is very small (much less than 0.1 dB) and can be neglected. Interestingly even on that level an indicator for a special effect in the cable can be seen as a sharp peak arises at 210 MHz.


Difference of S_{11} and S_{33}

As seen above in the single-ended measurements a huge peak in Delta RL, which is close to

10 dB, can be found at 210 MHz, exactly the frequency where we also find the peak in TCL.

This could be considered as the final cause of the peak but for balunless testing and single-ended measurements still more information can be accessed.
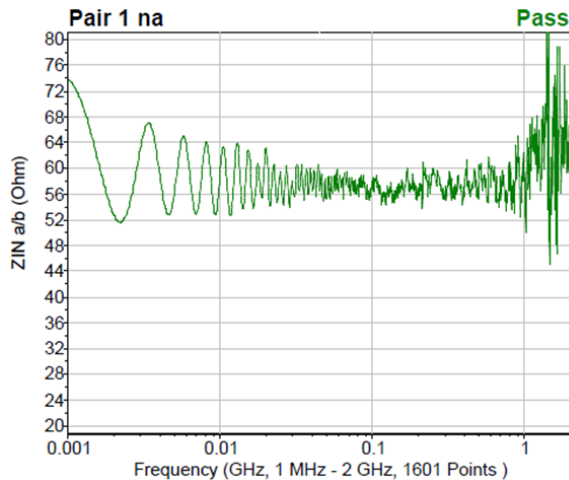
Single-ended Impedance of wire "a"
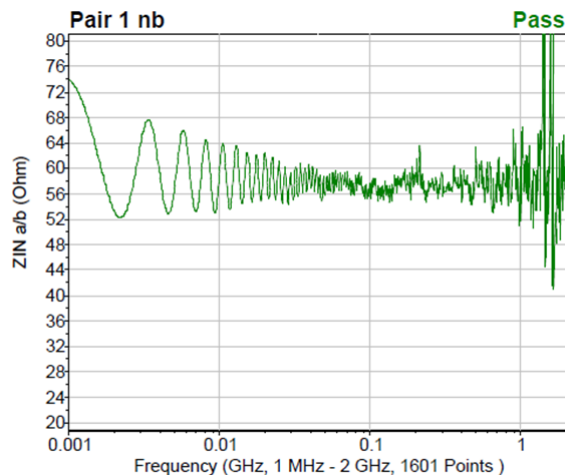
Single-ended Impedance of wire "b"

If we have the single-ended RL values it is a short way to get the single-ended impedance of each wire.

At the critical frequency of 210 MHz wire "a" forms a peak down as wire "b" goes directly in the opposite direction. This can be expected from the single-ended RL measurement but it is not clear which wire shows a higher impedance and which one a lower impedance.

This behaviour can now be interpreted. As well known, higher impedance means more distance between two electrical conductors, here repre-sented by the wire and the pair foil. Vice versa, lower impedance means less distance between the wire and the foil.

Finally it can be concluded that the mechanical structure of the pair is regularly, here approximately every meter, distorted during the production process in the wire extruder or afterwards during the stranding.

The sharp peak indicates that the mechanical problem is very stable, repeatable and probably easy to locate, e.g. related to the diameter of a pulley.

Case 3: IL ringing

We define IL ringing as percentage of deviation between IL measured and IL limit. Instead of a smooth line we find oscillating values.
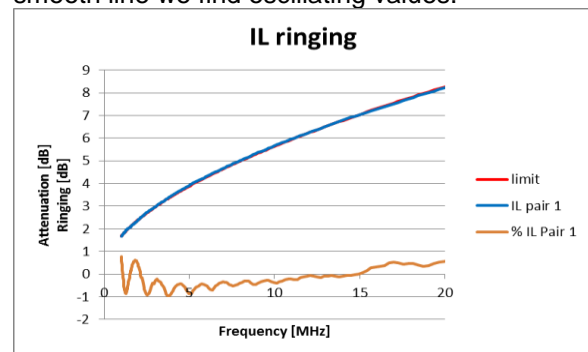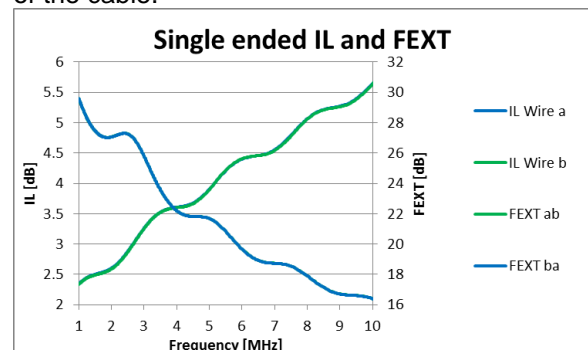

IL ringing at low frequencies

If we remember the transformation matrix we can find for IL (S_{dd21}) this formula:

$$S_{dd21} = \frac{1}{2}(S_{21} - S_{23} - S_{41} + S_{43})$$

The cause of IL ringing must be found in the single-ended S-parameters above, which are the Insertion Loss of wire "a" and wire "b", S_{21} and S_{43} respectively and inter pair FEXT S_{23} and S_{41}. Inter pair FEXT is the signal which is sent in at "a" wire and is received at "b" wire at the far end of the cable.


Single-ended IL and FEXT at low frequencies

All single-ended S-parameters have already some smooth waves but this is not the cause of

IL ringing. To understand the IL ringing we have to compare the differences between IL of "a" wire and "b" wire respectively the difference of inter pair FEXT.

As given in the graph below the differences are in a similar range of a few hundredth of dB. In this case we have to compare the absolute levels of single-ended IL and FEXT. The single-ended IL is close to the IL values of the cable, here between -2 dB and -6 dB for frequencies below 10 MHz. The FEXT values are much smaller, here between -30 dB and -16 dB for the same frequency range. In absolute values IL is higher than FEXT and has because of that a higher influence.
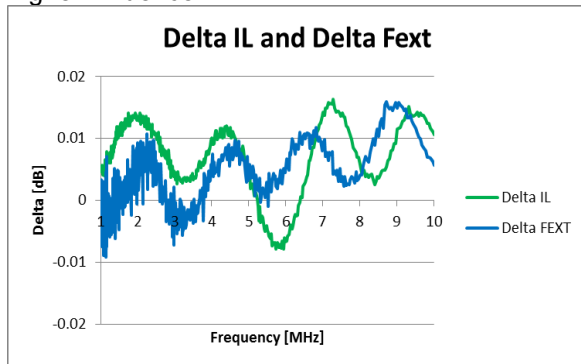
Delta IL end Delta FEXT

Are these values bad? What kind of values can be expected? Here the VNA specification can help. Each analyser is specified on transmission uncertainty. This value is typically between 0.02 dB and 0.05 dB.

Both values are clearly below the analyser specification. From that perspective we can consider the values as good and following this, the residual IL ringing is caused by the uncertainty of the used test equipment itself.
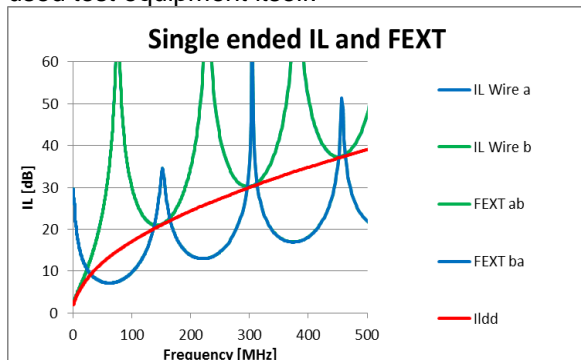
Single-ended IL and FEXT and differential IL

As additional information we can study the overlay of all graphs, the 4 single-ended measure-ments (blue and green) and the resulting differential IL (red).

Compared to the single-ended S-parameters differential IL is very smooth. Because of the differential data transmission we don't care about if the signals are received on the same wire of the pair or not.

But if we have a look at the graph then we see that for most frequencies the signal is received on the other wire at far end.

Conclusion

The new opportunities as presented in this paper open a door for better understanding of data cable manufacturing and providing some insights about the way how single-ended S-parameters can be used to understand weaknesses of cables better.
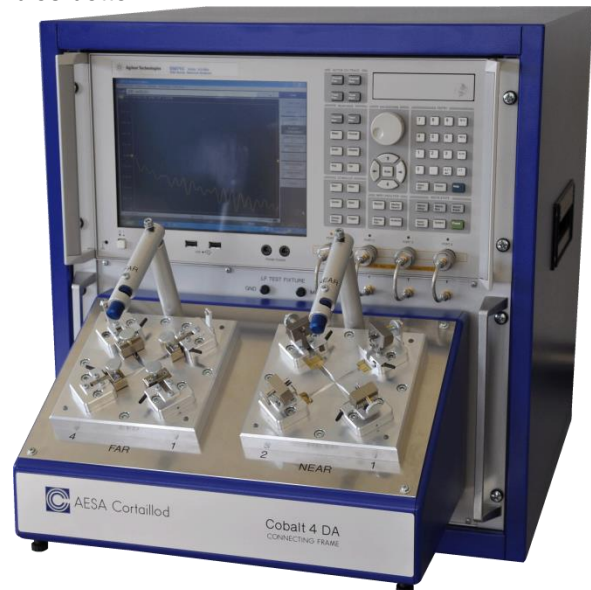
All shown measurements in this document are done with an AESA Cobalt system as shown above. It is fully automated balunless test equipment which fulfils the requirements of TIA°1183 and the upcoming TIA°1183-1 to test Category 8 cables and beyond.

Balunless testing is a great tool because it allows to access data from each single wire and how they are interacting in the pair. This technology allows analysing the cable also during production and sort out low performing pairs to reduce scrap and waste of material.

In such a way of thinking it helps to reduce development cost and reaction time, check and improve the quality during each production step and improve the factory's efficiency. Thanks to

such analysis a cable manufacturer can understand and control his production better and find weak points much faster.

As proven by many papers, mathematical superposition of single-ended S-Parameters is very accurate. Additionally to the well-known differential S-parameters we get also mixed-mode and common-mode S-parameters which are based on the same single-ended measurements but distinguished by the algebraic signs in the formulae.

Name	Abbreviation
Cable under Test	CUT
Device under Test	DUT
Equal Level Transverse Conversion Transfer Loss	EL TCTL
Insertion Loss	IL
Near End Crosstalk	NEXT
Far End Crosstalk	FEXT
Return Loss	RL
Transverse Conversion Loss	TCL
Vector Network Analyser	VNA

Abbreviations
References

Fan, W Lu, A C W Wai, L L and Lok, B K 2003, "Mixed-Mode S-Parameter Characterisation of Differential Structures", *Electronics Packaging Technology, 2003 5th Conference (EPTC 2003)*, STR/04/011/JT

Schweizer, D 2011, "Termination Strategy in Differential Measurements" as presented to Swiss National committees of TC46 and TC48

About the author

Peter Fischer joined AESA SA in August 2014 as R&D Project Manager. He holds a Bachelor of Science in Electrical engineering from Zurich University of Applied Sciences (ZHAW).

He published term and thesis papers in radio frequency technology under the titles '900 MHz synthesizer and modulator' and 'Wideband monitoring receiver'.

He formerly worked 6 years in the radio frequency lab, part of the development support department, at Reichle & De-Massari AG in Wetzikon, Switzerland.

Peter is member of IEC TC46, TC48 and CENELEC TC46X standardisation committees and its working groups, focused on data cables and test methods as balunless testing.

He holds a patent of a balunless adaptation for data cables.

[viii] Formula from Fan et al (2003)

All measurements were done with AESA Cobalt

---

[i] Drawing from IEC 61935-1

[ii] Drawing from IEC 61156-1-2 AMD 1

[iii] Drawing from Fan et al (2003)

[iv] Formula from Fan et al (2003)

[v] Drawing from Fan et al (2003)

[vi] Formula from Fan et al (2003)

[vii] Formula from Schweizer (2011)

AESA Cortaillod